Oxygen vacancy and photoelectron enhanced flexoelectricity in perovskite SrTiO$_3$ crystal ⊘

Yangshi Jin; Fan Zhang; Kai Zhou; Chun Hung Suen (ID) ; X. Y. Zhou ✉ (ID) ; Ji-Yan Dai ✉ (ID)

Check for updates

CrossMark

View Online

Export Citation

Articles You May Be Interested In

Mechanical tunability of flexoelectricity in elastomers

Appl. Phys. Lett. (September 2021)

Controllable semiconductor flexoelectricity by interface engineering

Appl. Phys. Lett. (November 2022)

Microstructure enhancement of macroscopic flexoelectric behavior of THV/Al composites

Journal of Applied Physics (April 2023)

21 August 2023 05:57:26

AIP Publishing

Oxygen vacancy and photoelectron enhanced flexoelectricity in perovskite SrTiO₃ crystal

Yangshi Jin,[1] Fan Zhang,[1] Kai Zhou,[2] Chun Hung Suen,[1] (iD) X. Y. Zhou,[2,a] (iD) and Ji-Yan Dai[1,3,a] (iD)

AFFILIATIONS

[1]Department of Applied Physics, The Hong Kong Polytechnic University, Hung Hom, Kowloon, Hong Kong, China
[2]College of Physics, Chongqing University, Chongqing 401331, China
[3]Guangdong-Hong Kong-Macao Joint Laboratory for Photonic-Thermal-Electrical Energy Materials and Devices, Research Institute for Smart Energy, The Hong Kong Polytechnic University, Hung Hom, Kowloon, Hong Kong, China

[a]Authors to whom correspondence should be addressed: xiaoyuan2013@cqu.edu.cn and Jiyan.dai@polyu.edu.hk

ABSTRACT

Photo-enhanced flexoelectricity or flexoelectricity-enhanced photovoltaic effect, named photo-flexoelectric, is an interesting topic and has application potential in photo-electro-mechanical devices. However, this effect is far from being well understood. In this work, we demonstrate the photoflexoelectric effect in perovskite-structured SrTiO₃ (STO) single crystal and reveal the coupling mechanism between its photovoltaic and flexoelectric effect. Driven by the flexoelectric field, light-induced electrons can tunnel through the Schottky junction at the Au/STO interface, giving rise to enhanced flexoelectricity, i.e., photoflexoelectric effect. Thermal annealing in vacuum induces oxygen vacancies in STO and results in stronger light absorption and enlarged photoflexoelectric effect.

Published under license by AIP Publishing. https://doi.org/10.1063/5.0047735

Flexoelectricity describes a material's electric polarization in response to a nonuniform strain. This effect was thought to be negligible for a long time due to its much smaller magnitude compared to other electromechanical effects such as piezoelectricity. However, many recent studies have largely expanded the flexoelectric effects from a simple polarization concept to a new modulation strategy in a wide range of functional materials,[1,2] therefore opening a new area of flexoelectronics.[3] The idea of utilizing flexo-polarization to tailor material's physical properties is attracting more attention because of a key fact: flexoelectricity is generated from a strain gradient and naturally accompanied by the symmetry breaking of the lattice.[4,5] This fact eliminates the restrictions like the Curie temperature in many piezoelectric materials and allows the existence and coupling with other physical properties in all materials from insulator to semiconductor as well as conductor.

The coupling between flexoelectricity and photovoltaics (PV), as one of the most promising phenomena from the application point of view, has triggered many investigations and discussions in the flexoelectric community. Yang *et al.* first raised the idea of flexo-photovoltaic effect, where the strain gradient-induced polarization in centrosymmetric materials could induce PV effect analogous to ferroelectric PV effect.[6] Later on, Shu *et al.* discovered that ultraviolet light (UV) can enhance the flexoelectricity by two orders of magnitude for

hybrid perovskites, and they further proved that such photo-flexoelectricity can be a general property of semiconductors.[7] Recently, controllable photoconductance in a freestanding BiFeO₃ membrane was demonstrated by Guo *et al.*,[8] extending the research of photoflexo-electric effect to thin films. Though there are more studies showing the effective coupling between flexoelectric and photoelectric properties, there still lacks a clear physical picture describing flexo-photovoltaic effect, where the interactions between photon, charge, and polarity make the mechanism more complicated.

As the photoflexoelectric effect has been observed in SrTiO₃ (STO),[6] this cubic structured perovskite could be a good platform to investigate the coupling between flexoelectricity and photovoltaics. We are also motivated by the fact that oxygen vacancy density in materials can influence their flexoelectric property; as reported, three orders of magnitude larger flexoelectric coefficient has been reported in reduced BaTiO₃ single crystal.[7] It is known that after high-temperature vacuum annealing, STO single crystal shows distinct electrical transport property change through the accumulation of oxygen vacancies.[9] Therefore, it is expected that stimulated by both light illumination and oxygen vacancies, a large flexoelectric response could be achieved in STO crystal.

In this work, we compared the pristine and high-temperature annealed STO single crystals' flexoelectricity and their response to

incident UV light, and we revealed coupling between the flexoelectric field, photo-induced current, and oxygen vacancy induced defects. These findings can help us to understand the mechanism of flexoelectricity and photoflexoelectric effect and may extend present solar cell technologies by enhancing the solar energy conversion efficiency from a wide pool of established semiconductors.[5] The increased flexoelectric coefficient may also have application prospects like energy harvesters,[10] light sensors,[11] and accelerometers.[12,13]

Two-side polished STO single crystals used in this work are from MTI Corporation, and the bare crystals were cut into a beam shape with a size of $5 \times 10 \times 0.5 \, mm^3$. Semitransparent gold electrodes of 5 nm thick were sputter deposited on the two surfaces of STO plates forming a capacitor structure (electrode/STO/electrode). To measure flexoelectricity, a piezoelectric actuator was used to deliver an oscillatory force to the free end of clamped cantilever-shaped crystals, and the alternating current induced by the oscillatory bending was measured with a lock-in amplifier connected to the electrodes with coaxial cables. Using standard elastic deformation equations, for a point-loaded single-clamped beam, the strain gradient was calculated from the deflection amplitude and the distance from the clamped side and actuator contact point, and the polarization was extracted from the amplitude of the oscillating current and the frequency of the actuator. The linear proportionality constant between polarization and strain gradient is the flexoelectric coefficient. To measure the photocurrent, the same setup was used, and the dc current induced by UV light was measured with a KEITHLEY 2400 source meter.

The u-bending and n-bending describe the bending geometry with the reference of the direction of light illumination, as illustrated

in Fig. 1, wherein both bending cases, light illuminates the top electrode. To introduce oxygen vacancies in STO, the bare crystals were thermally annealed in a $10^{-5} \, Pa$ vacuum at 700 °C for 2 h. As shown in Fig. 1, a slightly darker appearance can be seen from the annealed sample. A UV laser with 365 nm wavelength was used to induce the photoelectric effect, while the light intensity was calibrated with 3A-P-FS-12 (thermal power/energy laser measurement sensor) and StarLite P/N 7Z01565 (Low-Cost Portable Laser Power and Energy Meter).

The effective flexoelectric coefficient of (001) STO single crystal with semitransparent Au electrodes on both sides was measured in the dark and under UV light illumination. The polarizations under different strain gradients are shown in Fig. 1, where the labeled flexoelectric coefficients are calculated from the slope of the fitting lines. As shown in Figs. 1(a) and 1(b) which are for the n- and u-shape bending of the pristine STO crystal, respectively, the effective flexoelectric coefficient of the STO in the dark is about 1 nC/m. Under a vertical illumination by UV light from the top surface, as shown by the red lines in Figs. 1(a) and 1(b), the flexoelectric coefficients increase by a few times.

We then measured the effective flexoelectric coefficients of the annealed STO (or called reduced STO since XPS result reveals reduction of Ti^{4+} to Ti^{3+} as shown in Fig. S1), and the results are shown in Figs. 1(c) and 1(d). It is interesting to see that, compared to the pristine sample, the flexoelectric coefficient of the reduced STO shows one order of magnitude increment and a more significant enhancement under UV illumination. Integrating both effects from UV illumination and annealing, the flexoelectric coefficient of STO is greatly enhanced by more than two orders of magnitude, i.e., a strong photoflexoelectric effect which is independent of bending directions.
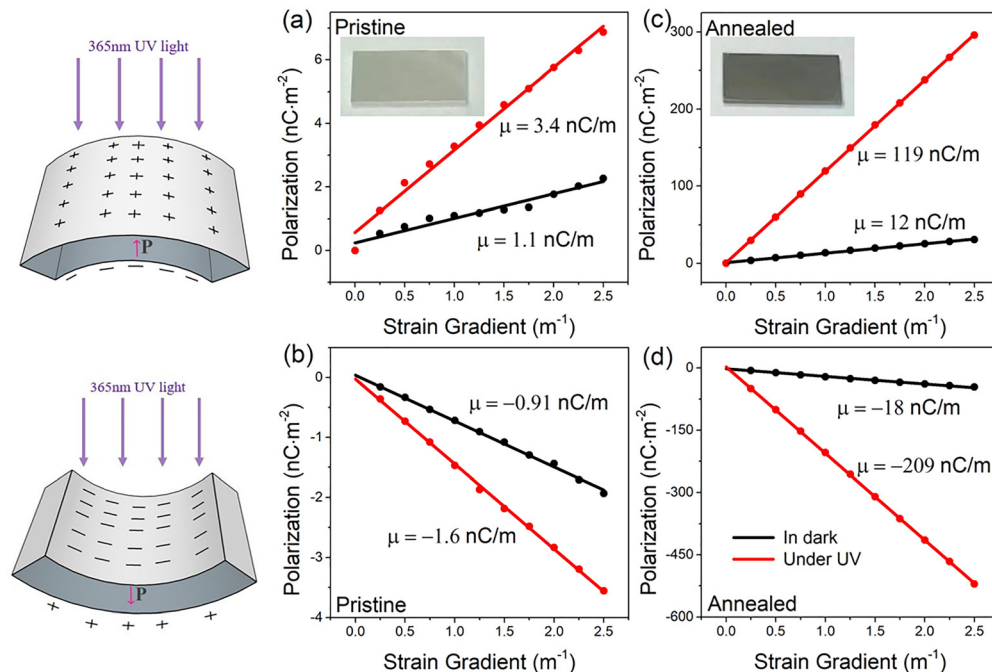

FIG. 1. Enhanced effective flexoelectric effect under UV light incident from the top surface of sample: (a) pristine STO under n bending, inset: the photo of the as-received pristine STO crystal, (b) pristine under u bending, (c) annealed STO sample under n bending, inset: the photo of the annealed STO crystal, and (d) annealed STO sample under u bending.

According to the barrier layer model,[14] the photoflexoelectric enhancement could be attributed to the narrowing of depletion width of the Schottky barrier at the Au/STO interface. In our experiment, both light illumination and induced oxygen vacancies can increase the charge carrier concentration in STO and further shrink the width of the depletion region. A quantitative dependence of the effective flexoelectric coefficient of semiconducting materials is given by[6]

$$\mu_{\mathrm{eff}} \equiv \sqrt{\frac{n\varepsilon_0\varepsilon_r}{2\phi_0}}\varphi\frac{t}{2}, \qquad (1)$$

where n is the free carrier concentration, ε_r the relative dielectric constant, ϕ_0 the Schottky barrier height, φ the surface deformation potential, and t the sample thickness. If we assume the change of the free charge carrier concentration dominates the change of μ_{eff} in our experiment, the flexoelectric enhancement for the reduced STO in the dark corresponds to two orders of magnitude increase in the free carrier concentration. As shown in Fig. 1, a much larger increment of μ_{eff} was observed on the annealed STO sample. This can be attributed to the presence of charged oxygen vacancies in the STO crystal, where the defect levels lower the Fermi level of STO and decrease the Schottky barrier at the interface and then result in a much higher μ_{eff} in Eq. (1).

We have conducted Hall measurement on the STO samples, but both pristine and 700 °C vacuum annealed samples show too high resistance for carrier concentration measurement. Alternatively, we measured the sheet carrier concentration of 550 °C annealed STO sample with AlN capping layer which is $1.2 \times 10^{15}/\mathrm{cm}^2$ at room temperature. This carrier concentration is generally within the range of the carrier concentration of the reduced STO substrate in a two-dimensional electron gas-like system.[15] It has been reported that 1200 °C vacuum annealing results in an average electron carrier concentration of $5 \times 10^{15}/\mathrm{cm}^3$, and it has also been demonstrated that when exposed to UV light, the electron carrier concentration in the annealed sample increases by two orders of magnitude.[16] Therefore, the increased electron carrier concentration in the annealed sample and its further boosting by UV light should be responsible for the increased flexoelectricity.

To understand the giant photo-flexoelectric increment more comprehensively, we studied the dependence of flexoelectric current on light intensity. As shown in Fig. 2, for both the pristine and annealed STO samples, the flexoelectric current increases gradually with the increase in the UV light intensity. The increase in flexoelectric current in correlation with UV light intensity increase suggests that the extra flexoelectric signal comes from the photo-excited carriers in the STO crystal. Furthermore, the nonlinear response of flexoelectric
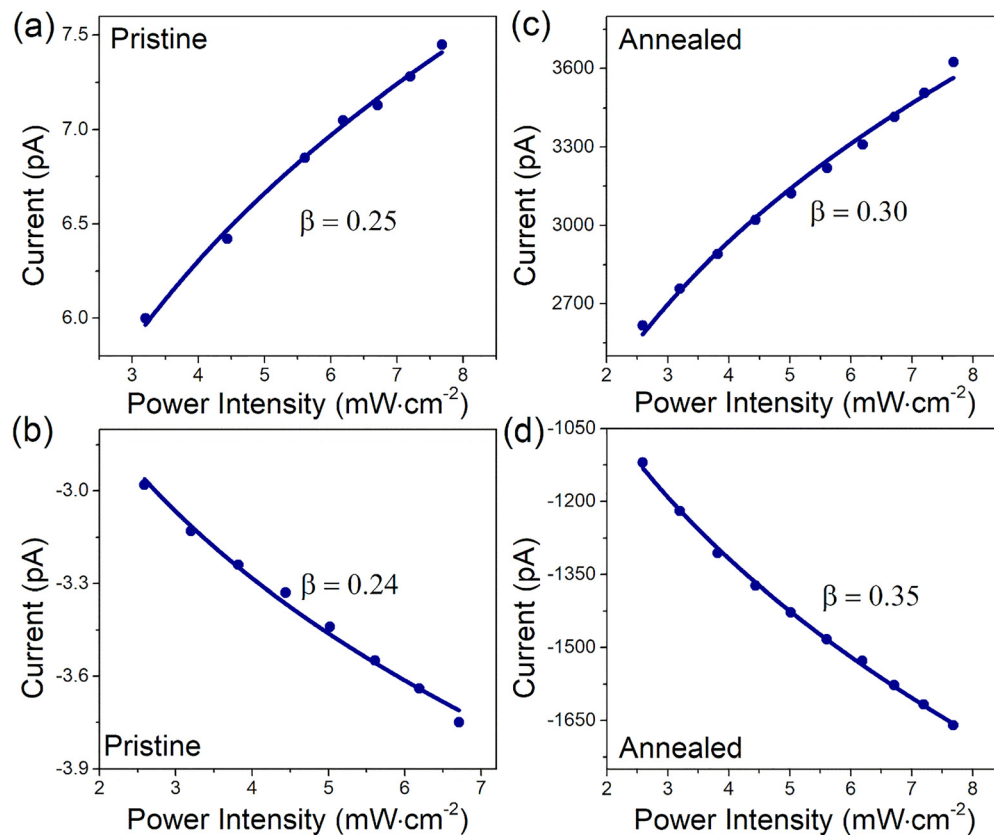

FIG. 2. Light-intensity dependence of flexoelectric current under a constant strain and increased UV light incident from top of the sample surface: (a) pristine STO under n bending, (b) pristine under u bending, (c) annealed STO sample under n bending, and (d) annealed STO sample under u bending. The fitting curves are with the power law.

21 August 2023 05:57:26

current fits well with the theory of photoresponse, which gives a power law

$$I = \alpha L^{\beta}, \qquad (2)$$

where α is a constant, L the light intensity, and β empirical power value related to the photosensitivity of the sample indicating the efficiency of generating charge carries by light.[17,18] From the fitting curve shown in Fig. 2, the β value is about 0.24–0.25 [Figs. 2(a) and 2(b)] for the pristine sample and 0.30–0.35 [Figs. 2(c) and 2(d)] for the annealed sample. The higher empirical power value of the annealed sample suggests that it is a more sensitive photoresponsivity than the pristine sample. Referring to Eq. (1), where the flexoelectricity is proportional to $n^{1/2}$ of the charge carrier density, if with $\beta = 0.25$ and 0.35, the photogenerated charge carrier densities should have a relationship with incident light intensity as $n \sim L^{0.5}$ and $L^{0.7}$, respectively, for the pristine and annealed samples. We note that such a nonlinear light-intensity-dependent property, i.e., the nonunity exponent, has also been observed in many nanostructure-based photodetectors, such as ZrS_2 nanoribbons,[19] CdTe nanoribbons,[20] CuO nanowires,[21] In_3S_3 nanowires,[22] etc., which is a result of the complex processes of electron–hole generation, trapping, and recombination in the semiconductor.[23,24]

To further demonstrate the generation of charge carriers in STO, we measured the photocurrent at the Au/STO interface, and the results are shown in Fig. 3. The generation of photocurrent when UV light incidents to the top surface is due to the Schottky junction formation at the interface of Au/STO, while the absorption of light (see Fig. S2) by the crystal makes the bottom surface of the crystal illuminated with much weaker light; therefore, the junction at top surface dominates the photocurrent (otherwise the symmetric electrodes on top and bottom will result in zero photocurrents).

It is well known that STO is a good insulator, but the positive photocurrent for the pristine STO suggests its weak p-type semiconducting nature due to the possible existence of Sr or Ti vacancies from nonperfect chemical stoichiometry during crystal growth at very high temperature. It has been reported that $1000\,^{\circ}C$ annealing can induce

Sr vacancies leading to p-type semiconducting of STO,[25–27] and the corresponding energy band diagram between Au and p-type STO is shown in Fig. 4(a).

It is interesting to see from Fig. 3 that the photocurrent of the reduced STO is two orders of magnitude larger than the pristine sample and the photocurrent is negative in contrast to the positive photocurrent for the pristine sample. The significant increase in photocurrent for the annealed sample is due to the oxygen vacancy induced defect levels as light absorption centers which convert photon energy to electron–hole pairs. The change of sign of the photocurrent can be understood by the fact that the annealed STO is an n-type semiconductor, which is well known, resulting in Schottky junction as shown in Fig. 4(b). In our experiment, the $700\,^{\circ}C$ annealing in a vacuum is a condition to reduce the STO crystal by introducing a large amount of oxygen vacancies. Oxygen vacancy induces the extra level $0.2\,eV$ below the conduction-band maximum (CBM) in the bandgap,[27] thus the STO crystal changes from p-type to n-type conducting.

It should be noticed that the photocurrent is a persistently decayed current under constant light and will not contribute to the alternative flexoelectric current measured by lock-in. However, as illustrated in Figs. 4(c) and 4(d), driven by the alternative flexoelectric field, light-induced electrons can tunnel through the Schottky junction at the Au/STO interface, giving rise to enhanced flexoelectricity, i.e., photo-flexoelectric effect. Flexoelectric polarization attracts photo-induced carriers and bending-induced electrons near the interface, resulting in a reduced interfacial energy barrier. This photo-enhanced flexoelectricity is independent of bending directions (n and u-shape bending) which can be seen in Figs. 1 and 2. On the other hand, we
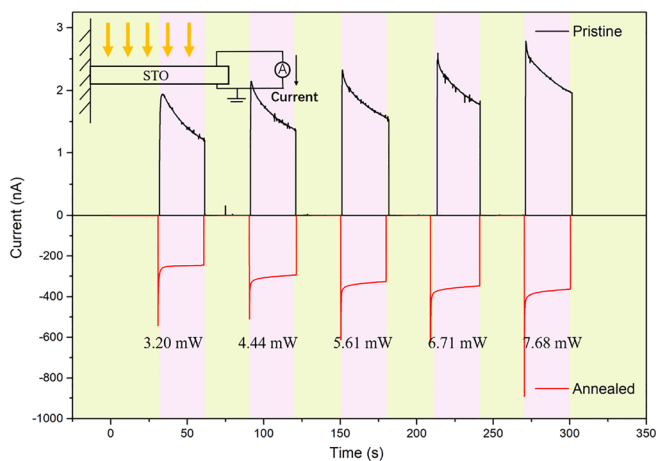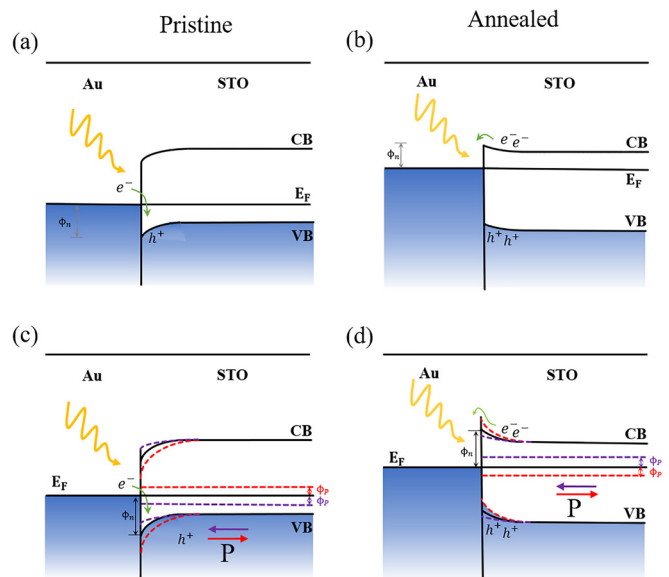
FIG. 3. Photocurrent of pristine and annealed STO samples. The annealed sample shows an enhanced and reversed photovoltaic effect.

FIG. 4. Energy band diagrams and electron tunneling at the Au/SrTiO₃ interface for pristine (a) and annealed (b) STO samples. (c) and (d) are the corresponding energy band diagrams and electron tunneling with the presence of flexoelectric polarization indicated by arrows. CB, energy pf conduction band minimum; VB, energy pf valence band maximum; E_{ϕ}, *vacuum energy*. P represents the flexoelectric field.

did not see a clear enhancement of the photovoltaic effect when we bent the sample; this is because the contribution of the flexoelectric field to the charge transfer across the Schottky junction is much smaller compared to the photocurrent which is two orders of magnitude larger than flexoelectricity induced current.

In summary, the photoflexoelectric effect has been studied in STO crystals. It is found that by introducing UV light stimulations and oxygen vacancies in STO, the effective flexoelectric coefficient can be enhanced by more than two orders of magnitude, comparing with the stoichiometry ones. These results help us to understand the mechanism of flexoelectricity and photoflexoelectric effect and may provide hints of more correlation effects between flexoelectricity and photon–charge interaction. The increased flexoelectric coefficient may also have application prospects like energy harvesters, light sensors, and accelerometers.

See the supplementary material for the XPS characterization to the annealed STO sample to confirm the formation of oxygen vacancies in STO. The light absorption spectrum of the STO sample with Au electrodes at the two surfaces was also measured to determine the optimal wavelength range.

AUTHORS' CONTRIBUTIONS

Y.J., F.Z., and K.Z. contributed equally to this work.

DATA AVAILABILITY

The data that support the findings of this study are available within the article and its supplementary material.

REFERENCES

[1]W. Ma and L. E. Cross, Appl. Phys. Lett. **86**(7), 072905 (2005).
[2]L. Liu, J. Mech. Phys. Solids **63**, 451 (2014).
[3]L. Wang, S. Liu, X. Feng, C. Zhang, L. Zhu, J. Zhai, Y. Qin, and Z. L. Wang, Nat. Nanotechnol. **15**(8), 661 (2020).
[4]P. Zubko, G. Catalan, and A. K. Tagantsev, Annu. Rev. Mater. Res. **43**, 387 (2013).
[5]F. Zhang, P. Lv, Y. Zhang, S. Huang, C.-M. Wong, H.-M. Yau, X. Chen, Z. Wen, X. Jiang, and C. Zeng, Phys. Rev. Lett. **122**(25), 257601 (2019).
[6]M.-M. Yang, D. J. Kim, and M. Alexe, Science **360**(6391), 904 (2018).
[7]L. Shu, S. Ke, L. Fei, W. Huang, Z. Wang, J. Gong, X. Jiang, L. Wang, F. Li, and S. Lei, Nat. Mater. **19**, 605 (2020).
[8]R. Guo, L. You, W. Lin, A. Abdelsamie, X. Shu, G. Zhou, S. Chen, L. Liu, X. Yan, and J. Wang, Nat. Commun. **11**(1), 2571 (2020).
[9]D. V. Christensen, M. von Soosten, F. Trier, T. S. Jespersen, A. Smith, Y. Chen, and N. Pryds, Adv. Electron. Mater. **3**(8), 1700026 (2017).
[10]X. Jiang, W. Huang, and S. Zhang, Nano Energy **2**(6), 1079 (2013).
[11]S. Huang, L. Qi, W. Huang, L. Shu, S. Zhou, and X. Jiang, J. Adv. Dielectr. **08**(02), 1830002 (2018).
[12]B. Wang, Y. Gu, S. Zhang, and L.-Q. Chen, Prog. Mater. Sci. **106**, 100570 (2019).
[13]W. Huang, S.-R. Kwon, S. Zhang, F.-G. Yuan, and X. Jiang, J. Intell. Mater. Syst. Struct. **25**(3), 271 (2014).
[14]J. Narvaez, F. Vasquez-Sancho, and G. Catalan, Nat. **538**(7624), 219 (2016).
[15]A. Ohtomo and H. Y. Hwang, J. Appl. Phys. **102**(8), 083704 (2007).
[16]M. C. Tarun, F. A. Selim, and M. D. McCluskey, Phys. Rev. Lett. **111**(18), 187403 (2013).
[17]S.-M. Huang, S.-J. Huang, Y.-J. Yan, S.-H. Yu, M. Chou, H.-W. Yang, Y.-S. Chang, and R.-S. Chen, RSC Adv. **7**(62), 39057 (2017).
[18]C. Lan, C. Li, Y. Yin, H. Guo, and S. Wang, J. Mater. Chem. C **3**(31), 8074 (2015).
[19]Y.-R. Tao, X.-C. Wu, and W.-W. Xiong, Small **10**(23), 4905 (2014).
[20]X. Xie, S.-Y. Kwok, Z. Lu, Y. Liu, Y. Cao, L. Luo, J. A. Zapien, I. Bello, C.-S. Lee, and S.-T. Lee, Nanoscale **4**(9), 2914 (2012).
[21]B. J. Hansen, N. Kouklin, G. Lu, I.-K. Lin, J. Chen, and X. Zhang, J. Phys. Chem. C **114**(6), 2440 (2010).
[22]X. Xie and G. Shen, Nanoscale **7**(11), 5046 (2015).
[23]M. Shaygan, K. Davami, N. Kheirabi, C. K. Baek, G. Cuniberti, M. Meyyappan, and J.-S. Lee, Phys. Chem. Chem. Phys. **16**(41), 22687 (2014).
[24]R.-S. Chen, H.-Y. Chen, C.-Y. Lu, K.-H. Chen, C.-P. Chen, L.-C. Chen, and Y.-J. Yang, Appl. Phys. Lett. **91**(22), 223106 (2007).
[25]V. M. Poole, C. D. Corolewski, and M. D. McCluskey, AIP Adv. **5**(12), 127217 (2015).
[26]L. Triggiani, A. B. Muñoz-García, A. Agostiano, and M. Pavone, Phys. Chem. Chem. Phys. **18**(41), 28951 (2016).
[27]T. Tanaka, K. Matsunaga, Y. Ikuhara, and T. Yamamoto, Phys. Rev. B **68**(20), 205213 (2003).